



Dose calculations – electron beam requirements for a pulsed radiography facility

Stanley Humphries, Ph.D.

Field Precision LLC

E mail: techinfo@fieldp.com

Internet: <https://www.fieldp.com>

1 Introduction

I was asked to calculate the required electron beam parameters to achieve the following dose values for a proposed pulsed radiographic facility:

A 6.0 MeV beam to produce a dose of 200 rad at a distance of 1.0 meter from the target.

An 8.0 MeV beam to produce a dose of 250 rad at 1.0 meter.

An 18.0 MeV beam to produce a dose of 1000 rad at 1.0 meter.

In all cases, the pulse length should be in the range 50 to 80 ns. A knowledge of the beam current is critical to assess the feasibility of different approaches. Experimental data from existing pulsed radiography facilities present some problems. Such measurements are difficult, and there is a wide range in reported results.

To start with a level playing field, I have calculated theoretical limits on the minimum beam current necessary to generate the target doses. I used an ideal electron beam with no energy spread, a point focus and zero emittance incident on a tungsten target. The calculations employed my Monte Carlo code **GamBet**, based on the **Penelope** radiation physics package. The package is used by several groups in Europe and has been well benchmarked. The solutions were performed in two stages:

1. The first set of calculations generated bremsstrahlung distributions for 1.0 A incident electron beams and addressed the choice of optimal target thickness.
2. In the following calculations, the photons were directed on an aluminum phantom for 80 ns to determine the deposited dose distribution. The results were extrapolated to 1.0 m assuming $1/d^2$ scaling.

2 Bremsstrahlung generation

The two-dimensional **GamBet** calculation employed cylindrical coordinates. A point beam of electrons with current $I = 1.0$ A moves in z at $r = 0.0$ mm. The beam strikes a tungsten plate of thickness Δ . The first step is to determine a useful thickness range. Clearly Δ must be less than the electron range R in the material. A target with $\Delta > R$ has higher self-absorption of the photons with no increase in bremsstrahlung output, while a thin target has low conversion efficiency. The implication is that there is a choice of thickness less than R that maximizes the forward X-ray flux. Table 1 lists

Table 1: Electron interactions with tungsten (NIST EStar site).

Kinetic energy (MeV)	R_{norm} (gm/cm ²)	Radiation yield	R (cm)
6.0	4.265	21.57%	0.2210
8.0	5.301	26.12%	0.2747
18.0	9.024	41.77%	0.4676

the normalized electron range, the total bremsstrahlung yield and the range for electrons in tungsten ($\rho = 19.3 \text{ gm/cm}^3$) for the three energies of interest. It should be noted that the range R is the integrated electron path length. Electrons undergo strong scattering; therefore, thin targets they follow a convoluted path that may actually reverse their direction. One implication is that the effective spot size for the diffusing electrons is comparable to the target thickness.

With scattering, the average distance of penetration into the target is less than the range. With this in mind, I investigated a set of target sheets with thicknesses from $\Delta = 0.1R$ to $\Delta = 0.7R$. For a thin target, the predicted mean angle of forward bremsstrahlung emission for a relativistic electron beam is approximately $1/\gamma$. With $\gamma = 12.74$ for 6.0 MeV electron, the predicted emission cone angle is about 4.5° . The emission angle for a thick target is considerably larger because of electron scattering.

I picked the following mesh dimensions for the 6.0 MeV calculations:

Along z , I set up a zone from 0.0000 mm to 1.5469 mm (the maximum target width) with 14 divisions to resolve the different sheet thicknesses.

I included an axial zone at coarse resolution that extended to 20.0 mm. This zone had the *Void* property in the **GamBet** calculation. The intention was to record photon positions in the escape file at 20.0 mm rather than at the target exit surface. The purpose will be apparent in the discussion of dose calculations in the following section.

The solution volume extended to 20.0 mm in the radial direction to capture photons created by scattered electrons.

Table 2 shows the script to control the **GamBet** run. The commands of the *Geometry* section load the mesh created from **TARGET60.MIN**, interpreting dimensions in cylindrical coordinates with units of mm. In the *Composition* section, Material 1 is set as tungsten and associated with Region 2. The *Source* section defines a mono-energetic point electron beam with 6.0 MeV

kinetic energy. For good statistics, I used 20,000 primaries. In the *Process* section, I set cutoffs to ignore photons and electrons with energy less than 50 keV and employed a bremsstrahlung forcing factor of 50.0.

The escape file **TARGET60ESC.SRC** for the run contained all the electrons, photons and positrons that left the solution volume. It was important to remove the electrons and positions because they would make a strong contribution to the downstream dose. I also wanted to find statistics for photons moving in the forward direction (*i.e.*, those that left the boundary at $z = 20.0$ mm with radius less than 10.0 mm). The filtering operation and distribution calculations were performed with the **GenDist** utility.

Results of the calculations as a function of target thickness are summarized in Tables 3, 4 and 5. Column 3 shows the average kinetic energy of electrons leaving the target (including knock-on electrons). Column 4 shows the energy sum over photons leaving the target in all directions divided by the incident electron beam energy. There is a broad maximum near $\Delta/R = 0.4$. The peak value is somewhat lower than the theoretical total yield because of photon absorption in the target. Column 4 shows the energy yield based on a sum of photons in the forward direction (within 26.5° of the z axis). The forward flux also has a maximum near $\Delta/R = 0.4$. The final column shows the average kinetic energy of forward-directed photons. The efficiency of radiation conversion increased at the higher energies. For all energies, the maximum in forward-directed flux occurred for a target thickness equal to about half the electron range, $\Delta/R \cong 0.5$.

3 Dose distributions

In the second set of calculations, the forward-directed photon distributions for $\Delta/R = 0.5$ entered a 10.0 aluminum block 20.0 mm from the target face. The witness plate was located relatively close to the target for good statistics. The resulting doses were then extrapolated to a distance of 1000.0 mm. The mesh defined by **TARGETDOSE.MIN** had a single aluminum region with a radial width of 10.0 mm. For convenience, the mesh extended from 0.0 mm to 10.0 mm in z . I picked an element size of 0.10 mm in z and 0.25 mm in r . The *Source* section of the **GamBet** input file **DOSE6005.GIN** for 6.0 MeV electrons had the following entries:

```
Shift 0.000 0.000 -19.999
SFile Target6005
NPMult = 50
TPulse: 80.0E-9
```

The *Shift* command subtracted 19.999 mm from the z coordinates of the photon so that they entered at the front face of the aluminum block. The

Table 2: Contents of the **GamBet** control script TARGET60.GIN.

```
GEOMETRY
  DUnit 1000.0
  GFile2D TARGET60.MOU Cylin
END

COMPOSITION
  Material W
  Region(1) = Void
  Region(2) = 1
END

SOURCE
  SList
    E 6.0E6 0.00001 0.00 0.00001 0.00 0.00 1.00 1.00
  End
  NPMult = 20000
END

PROCESS
  EAbs Electron 5.0E4
  EAbs Photon 5.0E4
  EAbs Positron 5.0E4
  C1 0.10
  C2 0.10
  WCc 5.0E4
  WCr -5.0E4
  DsMax(1) = 0.01
  Force Brems 50.0
END

ENDFILE
```

Table 3: 6.0 MeV beam, bremsstrahlung photon generation as a function of target thickness (theoretical total yield: 21.57%).

Δ/R	Δ (cm)	$\langle E_{elec} \rangle$ (MeV)	Total yield	Forward yield	$\langle E_{phot} \rangle$ (MeV)
0.1	0.0214	4.387	5.37%	2.072%	1.084
0.2	0.0429	2.969	11.06%	2.810%	1.081
0.3	0.0643	2.183	14.28%	3.201%	1.109
0.4	0.0857	1.721	15.44%	3.307%	1.113
0.5	0.1072	1.497	15.59%	3.284%	1.155
0.6	0.1286	1.470	15.20%	3.230%	1.205
0.7	0.1500	1.476	14.76%	3.158%	1.250

Table 4: 8.0 MeV beam, bremsstrahlung photon generation as a function of target thickness (theoretical total yield: 26.12%).

Δ/R	Δ (cm)	$\langle E_{elec} \rangle$ (MeV)	Total yield	Forward yield	$\langle E_{phot} \rangle$ (MeV)
0.1	0.2747	5.880	6.28%	2.92%	1.525
0.2	0.5494	3.931	12.91%	4.07%	1.507
0.3	0.8241	2.759	17.31%	4.57%	1.481
0.4	1.0988	2.131	19.11%	4.80%	1.482
0.5	1.3735	1.752	19.56%	4.85%	1.512
0.6	1.6482	1.616	19.14%	4.69%	1.538
0.7	1.9229	1.580	18.69%	4.61%	1.577

Table 5: 18.0 MeV beam, bremsstrahlung photon generation as a function of target thickness (theoretical total yield: 41.77%).

Δ/R	Δ (cm)	$\langle E_{elec} \rangle$ (MeV)	Total yield	Forward yield	$\langle E_{phot} \rangle$ (MeV)
0.1	0.4676	12.050	9.90%	6.83%	3.516
0.2	0.9352	7.965	18.85%	10.17%	3.349
0.3	1.4028	5.618	25.94%	11.80%	3.225
0.4	1.8704	4.192	30.37%	12.43%	3.121
0.5	2.3380	3.406	32.14%	12.56%	3.043
0.6	2.8056	2.968	32.40%	12.45%	3.008
0.7	3.2732	2.758	31.71%	12.17%	3.003

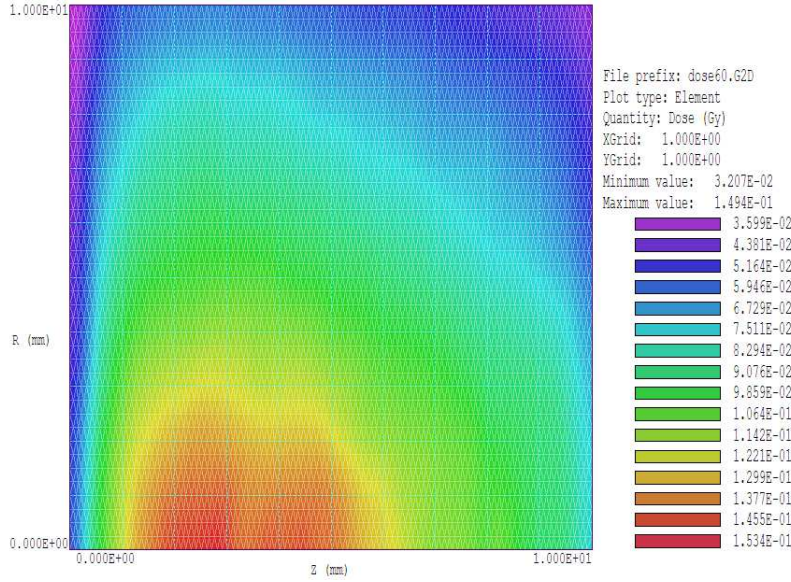


Figure 1: Dose in an aluminum phantom, bremsstrahlung photons created by a 6.0 MeV, 1.0 A beam.

value of *NpMult* initiated 50 showers for each of the 177,482 primary photons for good statistics. The value of *TPulse* specified an 80 ns pulse length for the photon flux. With this choice, the dose values were recorded in Gy (grays) rather than as a dose rate (Gy/s). Figure 1 plots the resulting smoothed dose distribution. The figure shows that some care must be taken in the definition of dose. Because of the buildup of knock-on electrons, the surface dose is significantly lower than the peak value (hence the use of intensifier screens in radiography).

The peak dose of 0.153 Gy (15.3 rad) occurs on-axis at a depth of 2.5 mm (an effective distance of 2.25 cm from the target face). The peak dose per ampere of beam current at a distance of 100.0 cm is

$$D(100) = 15.3 \left(\frac{2.25}{100.0} \right)^2 = 7.75 \text{ mrad/A.} \quad (1)$$

The required beam current for a dose of 200 rad is therefore $I = 25.8 \text{ kA}$.

The results are based on the assumption that there is vacuum between the exit of the target and the aluminum witness plate. Suppose the space is actually filled with air and we want to estimate the effect on the photon distribution at a distance of 1.0 m. One strategy is to fill the 20 mm void with air at 50 times normal density. The special material can be defined with the alternate form of the **GamBet** *Material* command:

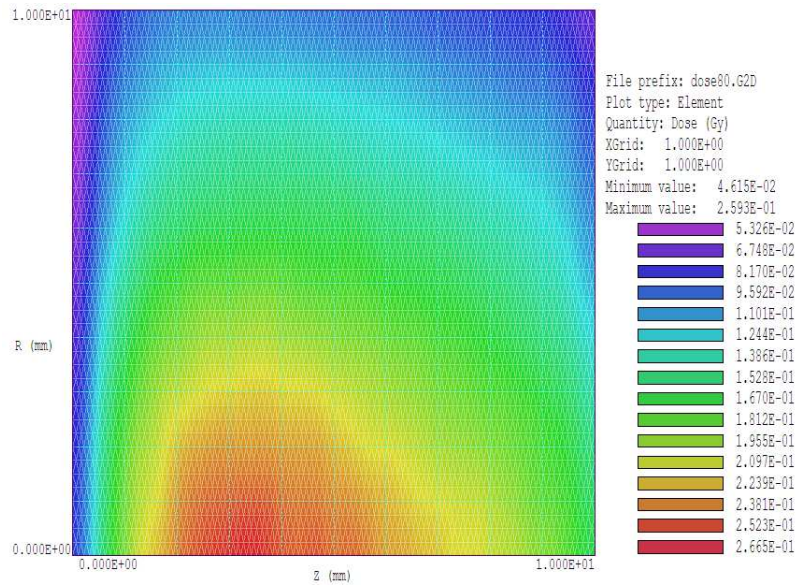


Figure 2: Dose in an aluminum phantom, bremsstrahlung photons created by an 8.0 MeV, 1.0 A beam.

Material

Name Air50
 Component N 0.80
 Component O 0.20
 Density: 0.06145
 Insulator

End

A check of the photon distribution in the filtered escape file shows that the effect of the air is relatively small. The number of photons drops from 178,842 to 178,669 and the average energy changes from 1.108 MeV to 1.106 MeV.

Figures 2 and 3 show the dose distribution for the 8.0 and 18.0 MeV beams. The doses are higher and the peak position moves to a greater depth in the phantom. At 8.0 MeV, the peak dose of 26.7 rad occurs at a depth of about 3.2 mm, while the peak dose is 116.0 rad at 4.5 mm depth for an 18 MeV beam. An analysis similar to that for the 6.0 MeV beam shows that a beam current of 17.4 kA is required for 8.0 MeV beam energy to generate a dose of 250 rad at 1.0 m. The beam current for a dose of 1000 rads at 1.0 m for an 18.0 MeV beam is 14.4 kA.

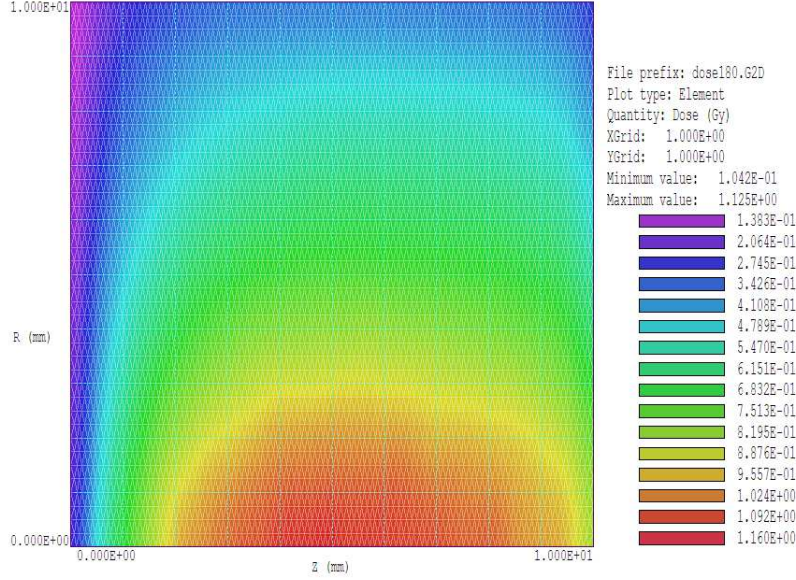


Figure 3: Dose in an aluminum phantom, bremsstrahlung photons created by an 18.0 MeV, 1.0 A beam.

4 Effect of target material

Tantalum is sometimes used instead of tungsten as an X-ray target for mechanical reasons. Tantalum has $Z = 73$ (compared to $Z = 74$ for tungsten) and has density $\rho = 16.654 \text{ gm/cm}^3$. I repeated the 8.0 MeV calculations with a tantalum target to make a comparison. The results tabulated in Table 6 are close to those of Table 4. A dose calculation yields 26.8 rad at 3.2 mm depth. The implication is that there is no statistically-significant difference in radiation production with a tantalum target. The lower density is balanced by a longer electron range and increased target thickness. Figure 4 shows equi-dose contours in a large aluminum phantom with front face 20.0 mm from the tantalum target.

Table 6: 8.0 MeV beam, bremsstrahlung photon generation as a function of target thickness, tantalum target (theoretical total yield: 25.84%).

Δ/R	Δ (cm)	$\langle E_{elec} \rangle$ (MeV)	Total yield	Forward yield	$\langle E_{phot} \rangle$ (MeV)
0.1	0.318	5.902	6.19%	2.93%	1.519
0.2	0.636	3.962	12.82%	4.02%	1.491
0.3	0.954	2.815	17.10%	4.57%	1.470
0.4	1.272	2.128	19.05%	4.81%	1.474
0.5	1.590	1.749	19.48%	4.80%	1.494
0.6	1.908	1.595	19.03%	4.74%	1.528
0.7	2.226	1.562	18.62%	4.63%	1.565

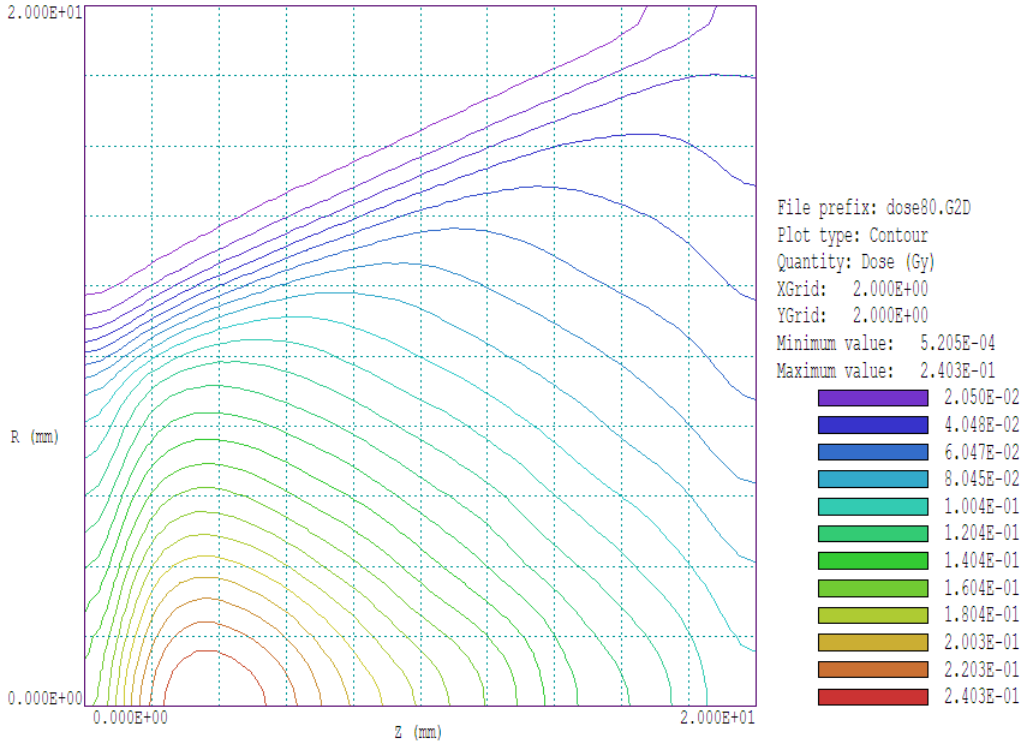


Figure 4: Contours of dose distribution, large phantom, tantalum target, 8.0 MeV electrons.

5 Conclusions

The calculated values are for the minimum current to achieve the dose requirements. The beam current must be larger for non-ideal beams with an extended spot size and non-zero emittance. In particular, electrons from a pinched-beam diode have a high angular divergence which would increase the angular spread for forward emission. My main conclusion is that the radiography requirements are ambitious. Although current levels of 20 kA are easily achieved with a pulsed-power generator coupled to a pinched-electron-beam diode, voltages of 6.0 to 8.0 MV may translate into large, costly devices. A linear induction accelerator may be required to reach a beam energy of 18 MeV. To put the challenge in perspective, a 14 kA beam current is about five times higher than the operating level of the DARHT II accelerator.